CDDpress

www.nature.com/cdd

ARTICLE

Check for updates

Brain-specific Pd1 deficiency leads to cortical neurogenesis defects and depressive-like behaviors in mice

Fen Ji[1,2,3]✉, Chao Feng[1,3,4], Jie Qin[1,3,4], Chong Wang[1,5], Dongming Zhang[1,3], Libo Su[1], Wenwen Wang[1], Mengtian Zhang[1,3], Hong Li[1,2], Longbing Ma[6], Weicheng Lu[7], Changmei Liu[1,2,3], Zhaoqian Teng[1,2,3], Baoyang Hu[1,2,3], Fengzeng Jian[6]✉, Jingdun Xie[7]✉ and Jianwei Jiao[1,2,3]✉

Embryonic neurogenesis is tightly regulated by multiple factors to ensure the precise development of the cortex. Deficiency in neurogenesis may result in behavioral abnormalities. Pd1 is a well-known inhibitory immune molecule, but its function in brain development remains unknown. Here, we find brain specific deletion of *Pd1* results in abnormal cortical neurogenesis, including enhanced proliferation of neural progenitors and reduced neuronal differentiation. In addition, neurons in *Pd1* knockout mice exhibit abnormal morphology, both the total length and the number of primary dendrites were reduced. Moreover, $Pd1^{cKO}$ mice exhibit depressive-like behaviors, including immobility, despair, and anhedonia. Mechanistically, Pd1 regulates embryonic neurogenesis by targeting Pax3 through the β-catenin signaling pathway. The constitutive expression of Pax3 partly rescues the deficiency of neurogenesis in the *Pd1* deleted embryonic brain. Besides, the administration of β-catenin inhibitor, XAV939, not only rescues abnormal brain development but also ameliorates depressive-like behaviors in $Pd1^{cKO}$ mice. Simultaneously, Pd1 plays a similar role in human neural progenitor cells (hNPCs) proliferation and differentiation. Taken together, our findings reveal the critical role and regulatory mechanism of Pd1 in embryonic neurogenesis and behavioral modulation, which could contribute to understanding immune molecules in brain development.

Cell Death & Differentiation (2023) 30:2053–2065; https://doi.org/10.1038/s41418-023-01203-3

INTRODUCTION

Embryonic neurogenesis, including the proliferation, differentiation, migration and lamination of the developing neural cells, is essential for the architectural formation and functional implementation of the nerves system. Deficiency in neurogenesis may result in behavioral abnormalities. Major depressive disorder (MDD), a widespread mental disorder, is the leading cause of disabilities in humans. The pathophysiology of depression is not comprehensively elucidated. Reduced hippocampus volume is one typical neurological characteristic of MDD, which may be caused by a decline in neurogenesis and neuroplasticity [1]. Growing evidence showed that similar neural alterations are also found in early-onset depression [2]. It is unclear whether embryonic neurogenesis contributes significantly to the onset of MDD.

To ensure the precise development of the nervous system, embryonic neurogenesis is spatially and temporally regulated by multiple factors. Many factors that are well-known in the immune system are also expressed in the nervous system and played nonimmune functions in normal brain development. For example, proinflammatory cytokines TNF-α [3, 4]and IL-6 [5], complement C1q and C3 [6], members of the major histocompatibility complex class I (MHCI) [7] are expressed in neurons and involved in synaptic plasticity during brain development. CD93 expressed in neural stem cells and neurons is a negative regulator for the output of astrocytes. Mice lacking CD93 exhibit autistic-like behaviors [8]. A recent study has demonstrated that brain-specific deficiency of STING results in abnormal embryonic neurogenesis and autistic-like behaviors in mice [9]. Most of the research focuses on the regulation of immune proteins on the later neurodevelopment, such as the establishment and connections of synapses. Although numerous immune proteins are also expressed in the neural progenitor cells, the effect of immune protein in early embryonic neurogenesis is not well illustrated.

Programmed cell death protein 1 (PD-1), a member of the CD28 superfamily, is a well-known immunotherapies target. After binding with it's mainly ligands PD-L1, PD-1 is activated and thus inhibits T cell proliferation, activation, and cytokine production. Now Checkpoint inhibitor-based immunotherapies that target Pd1 have achieved unprecedented success in the treatment of different cancer types. Although the immunological functions of Pd1 have attracted broad attention, the neurological function of Pd1 remains less unknown. Previous reports showed that PD1 is expressed in mouse neurons and has a role in inhibiting acute and

[1]State Key Laboratory of Reproductive Biology, Institute of Zoology, Chinese Academy of Sciences, 100101 Beijing, China. [2]Innovation Academy for Stem Cell and Regeneration, Chinese Academy of Sciences, 100101 Beijing, China. [3]University of Chinese Academy of Sciences, 100049 Beijing, China. [4]Sino-Danish College at University of Chinese Academy of Sciences, 100049 Beijing, China. [5]School of Life Sciences, University of Science and Technology of China, Hefei 230026 Anhui, China. [6]Department of Neurosurgery, Xuanwu Hospital, Capital Medical University, 100053 Beijing, China. [7]Department of Anesthesiology, Sun Yat-sen University Cancer Center, Guangzhou 510060 Guangdong, China. ✉email: jifen@ioz.ac.cn; jianfengzeng@xwh.ccmu.edu.cn; xiejd6@mail.sysu.edu.cn; jwjiao@ioz.ac.cn

Received: 9 November 2022 Revised: 18 July 2023 Accepted: 2 August 2023
Published online: 8 August 2023

chronic pain [10]. The blockade of Pd1 can enhance the memory of Alzheimer's disease mice [11]. Pd1 is located at the long (q) arm of chromosome 2. The deletion of this specific region causes a chromosome disease, 2q37 deletion syndrome. Patients with this syndrome exhibit neurological abnormalities, including mild to severe intellectual disability and autistic behavior [12]. All the reports indicate that Pd1 play an essential role in nerves system, the function of Pd1 in embryonic neurogenesis remains unknown.

In this study, we explore the neurological function of Pd1 in brain development. Pd1 is broadly expressed in the membrane of neural progenitor cells and neurons. Ablation of Pd1 results in impaired embryonic neurogenesis, including enhanced neural progenitor proliferation, reduced neural differentiation and delayed neuron migration. Neurons showed aberrant dendrite development when Pd1 is suppressed. Pd1 deficiency mice exhibit depressive-like behaviors. The neurological function of Pd1 is performed by targeting Pax3 through regulation of the β-catenin/GSK3β signaling pathway.

RESULTS

Pd1, not Pdl1, regulates the development of embryonic cerebral cortex

Pd1 expressed in the development of embryonic cerebral cortex, peaked at E13-E15, which coincided with the period of active neurogenesis and gradually decreased after E15 (Fig. 1A). The expression of Pdl1 had no significant difference during the development proceeds (Fig. 1A). In the embryonic cerebral cortex, Pd1 and Pdl1 were broadly expressed in the membrane of neural cells (Fig. 1B, C), including nestin-positive neural progenitors residing in the ventricular zone (VZ)/subventricular zone (SVZ) (Fig. 1D, E) and Tuj1-positive neurons in the cortical plate (CP) (Fig. 1F). Simultaneously, we found Pd1 and Pdl1 were expressed in neural progenitors labeled by Nestin and Tbr2 and neurons labeled by Tuj1 in vitro (Supplementary Fig. S1A, B). The expression of Pd1 in precursor and neurons was further detected by RT-PCR. Results showed Pd1 is expressed both in precursor and neurons (Supplementary Fig. S1C).

Based on Pd1 and Pdl1 expression in the cerebral cortex, we next explore the potential role of Pd1 and Pdl1 in brain development. Short hairpin RNAs (shRNAs) targeting the coding region of Pd1 and Pdl1 were constructed to silence the expression of Pd1 and Pdl1 respectively. The specificity of shRNAs was verified by western blot. The results showed that the expression of endogenous Pd1 was reduced in primary neural progenitor cells (NPCs) infected with two specific shRNA lentiviruses (Supplementary Fig. S1D) and obviously increased in NPCs infected with Pd1 overexpressing lentivirus (Supplementary Fig. S1E). Consistently, exogenous Flag-Pd1 was also significantly up-regulated in Flag-Pd1 transfected 293FT cells (Supplementary Fig. S1F). Pdl1 is also down-regulated by Pdl1-shRNA and up-regulated by Flag-Pdl1 (Supplementary Fig. S1G–J).

To investigate the regulation of Pd1 on brain development, control or Pd1 shRNA plasmids were electroporated together with a GFP plasmid into E13 mouse brains, and then the brains were harvested 2 days later. Compared with control, the inhibition of Pd1 resulted in abnormal positioning of GFP-positive cells in the embryonic mouse cortex. An obvious increase of GFP-positive cells in the VZ/SVZ and a corresponding reduction of GFP-positive cells in the CP were investigated (Fig. 1G, H). These results indicate that Pd1 plays an essential role in cortical development.

To explore the impact of Pdl1 expression during neural development, control or Pdl1 shRNA plasmids mixed with a GFP plasmid were introduced into E13 mouse brain by in utero electroporation experiments. No obvious difference was found in the distribution of GFP-positive cells upon Pdl1 suppression (Supplementary Fig. S2A, B). The result promoted us to perform the reciprocal Pdl1 gain-of-function experiment. Consistently, overexpression of Pdl1 also had no evident effect on brain development (Supplementary Fig. S2C, D). The proliferated NPCs labeled by BrdU and mitotic NPCs labeled by pH3 had no obvious variation when Pdl1 was silenced (Supplementary Fig. S2E–H). To test whether Pdl1 has effect on neuronal differentiation, electroporated brain sections were subjected to immunostaining with neuronal marker, Tuj1. The result showed that the ratio of GFP^+Tuj1^+cells in GFP^+ cells have no significant difference, indicating the silence of Pdl1 has no obvious impact on neuronal differentiation (Supplementary Fig. S2I, J). Taken together, these results suggest that pd1 knockdown, not pdl1 knockdown causes abnormal cortical development.

Given abnormal GFP^+ cell distribution was observed in the developed brain, we next explore the function of Pd1 in the proliferation and differentiation of cortical progenitors. To gain insight into the role of Pd1 in proliferation, BrdU was injected into the pregnant dams to label the cycling neural progenitors 2 h before the electroporated brains were collected. Compared with the control, more BrdU incorporation was observed in the GFP^+ cells upon Pd1 knockdown (Supplementary Fig. S3A, B), indicating that Pd1 is required for the proliferation of neural progenitors in vivo. To test the impact of Pd1 on neural differentiation, cell cycle exit experiment was performed. The number of cells that exited the cell cycle were reduced when Pd1 was inhibited (Supplementary Fig. S3C, D). Simultaneously, the proportion of cells that were positive for the neuronal marker Tuj1 was decreased upon Pd1 knockdown (Supplementary Fig. S3E, F). To determine the regulation of Pd1 on NPCs proliferation and the following neuronal differentiation, BrdU birth-dating experiment was performed. The brains electroporated at E13 were labeled by BrdU at E14 and harvested at E18 (Supplementary Fig. S3G). As BrdU is permanently labeled at the final mitotic division of NPCs, the differentiation and migration of labeled NPCs can be further traced. Compared with the control, the number of newborn neurons labeled by BrdU and GFP was decreased in CP when Pd1 was silenced (Supplementary Fig. S3H, I). When Pd1 was overexpressed, the percentage of GFP^+ cells are decreased in VZ/SVZ and increased in CP (Supplementary Fig. S4A, B). More GFP^+ cells were labeled by Tuj1, indicating that Pd1 promotes neuronal differentiation (Supplementary Fig. S4C). Simultaneously, the proliferated NPCs labeled by Ki67 (Supplementary Fig. S4D, E) or pH3 (Supplementary Fig. S4F, G) were reduced. Together, these results suggest the involvement of Pd1 in embryonic neurogenesis.

Brain-specific deletion of Pd1 impairs neurogenesis

To circumvent the possibility of Pd1 shRNA being off-target, we next examined whether brain-specific deletion of Pd1 could recapitulate the phenotypes observed in PD-1 shRNA. For this purpose, we generated a mouse strain carrying a Pd1 conditional knockout allele by targeting the deletion of exon 2 to exon 4 ($Pd1^{fl/fl}$). To specifically ablation the function of Pd1 in the nervous system, $Pd1^{fl/fl}$ mice were crossed with *Nestin-Cre* mice (Fig. 2A). Western blot showed that the expression of Pd1 was significantly reduced when Pd1 was loss (Fig. 2B). To verify the role of Pd1 in embryonic neurogenesis, GFP plasmid were electroporated at E13 and the brains were harvested at E16. Consistent with the results of Pd1knockdown, a marked increase in GFP^+ cells in the VZ/SVZ and IZ was investigated in $Pd1^{cKO}$ mice, and there was a significant reduction in GFP^+ cells in the CP (Fig. 2C, D). Compared with $Pd1^{fl/fl}$ mice, the number of $BrdU^+$ (Fig. 2E, F) and $pH3^+$ cells (Fig. 2G, H) were increased in the VZ/SVZ of $Pd1^{cKO}$ mice. Meanwhile, the size of neurospheres generated from E12 $Pd1^{cKO}$ progenitors was increased (Fig. 2I, J). Correspondingly, the immunostaining exhibited an increase in the number of $Tbr2^+$ progenitors and a decrease in the neuronal differentiation in the VZ of $Pd1^{cKO}$ mice at E16 (Fig. 2K, L). Consistently, the number of $Ctip2^+$ neurons was also decreased when *Pd1* was deleted (Fig. 2M, N). These results indicate that the brain-specific deletion of Pd1 impairs embryonic neurogenesis.

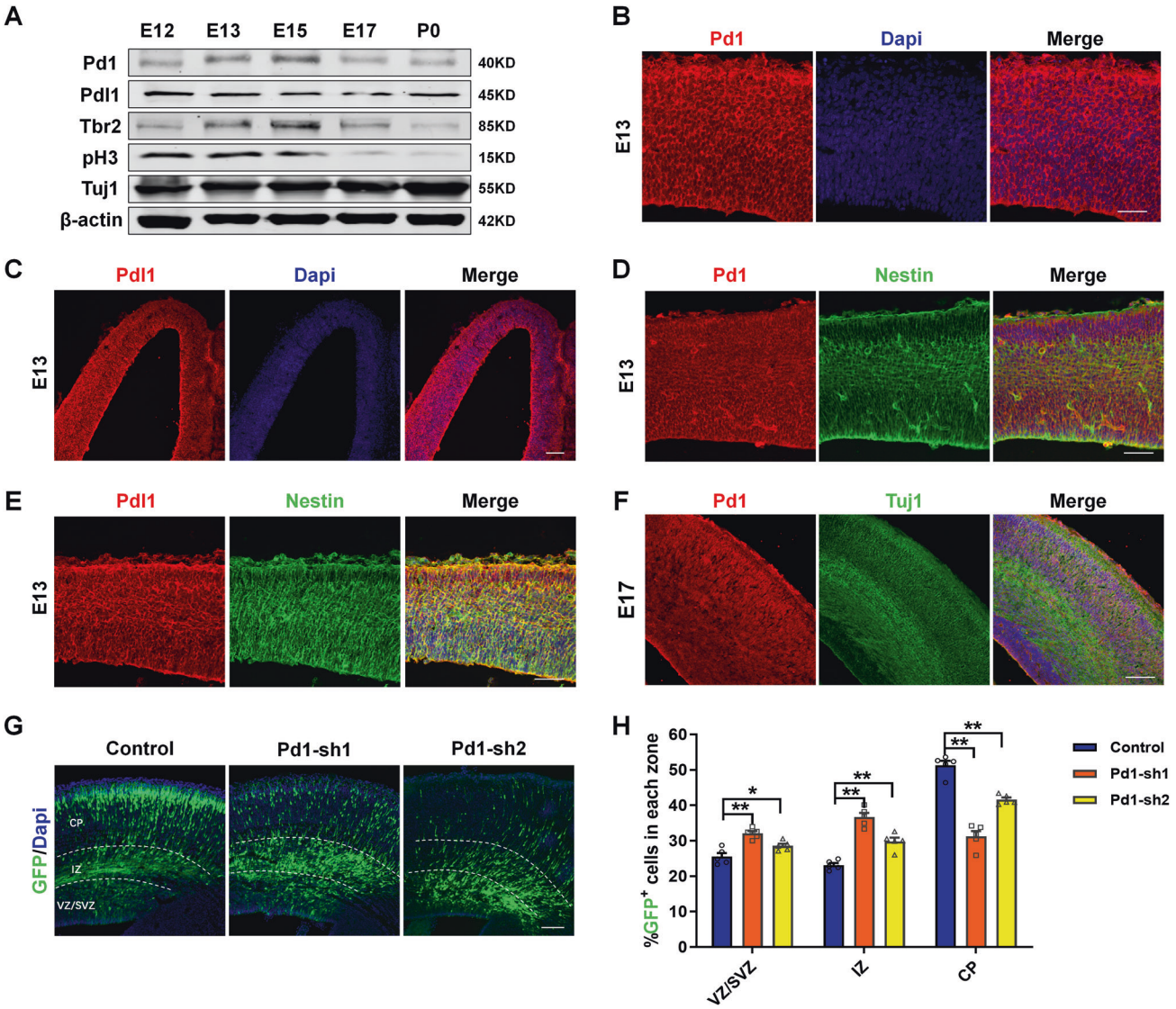

Fig. 1 Pd1 is expressed in the embryonic brain and involves in the regulation of neurogenesis. A Western blot analysis shows Pd1 is expressed in the development of the cerebral cortex. Brains at E12, E13, E15, E17, and P0 were collected and subjected to western blotting. Lysates were immunoblotted with antibodies for Pd1, Pdl1, Tbr2, pH3, Tuj1, and β-actin. $n = 3$ individual experiments. **B** Images of E13 embryonic mouse brain sections stained for Pd1 and Dapi. $n = 5$ individual experiments. **C** Images of E13 embryonic mouse brain sections stained for Pdl1 and Dapi. $n = 5$ individual experiments. **D** Pd1 is co-labeled with Nestin at E13. n = 5 individual experiments. **E** Pdl1 is co-labeled with Nestin at E13. $n = 5$ individual experiments. **F** Pd1 is expressed in the membrane of neurons labeled with Tuj1 at E17. $n = 5$ individual experiments. **G** Pd1 knockdown causes abnormal GFP^+ cell distribution in the developing neocortex. Control, Pd1-sh1, and Pd1-sh2 plasmids were electroporated into the embryonic brain at E13. The brains were harvested at E16 and then sliced into sections for analysis. **H** Graph shows the percentage of GFP^+ cells in the VZ/SVZ, IZ, and CP. VZ/SVZ ventricular zone/subventricular zone, IZ intermediate zone, CP cortical plate. Error bars represent means ± S.E.M.; Two-tailed unpaired t-test, $P < 0.05$(*), $P < 0.01$(**), n.s. not significant. The scale bar represents 100 μm.

In addition to Pd1 conditional knockout mice, Pd1 knockout mice were also generated to deplete the expression of Pd1. Compared with $Pd1^{+/+}$ mice, a striking alteration of electroporated cell distribution was observed in $Pd1^{-/-}$ mice. Most GFP^+ cells were located in VZ/SVZ and IZ. Almost no GFP cells were in CP (Supplementary Fig. S5A, B). Correspondingly, the percentage of $pH3^+$ cells was increased (Supplementary Fig. S5C, D) and $Tuj1^+GFP^+$cells in GFP^+ cells was reduced (Supplementary Fig. S5E, F) in $Pd1^{-/-}$ mice. These results further support the essential role of Pd1 in embryonic cortical development. To test whether astrocytes and oligodendrocytes are affected when *Pd1* is lost, the expression of ALDH1L1, a marker of astrocyte, and Oligo2, a marker of oligodendrocyte, were detected by western blotting. The results showed that no significant difference was found between $Pd1^{fl/fl}$ and $Pd1^{cKO}$ mice brains (Supplementary Fig. S5G, H), indicating the astrocytes, and oligodendrocytes are not affected by *Pd1* loss.

Down regulation of Pd1 impeded the migration of cortical neurons during development

To study the potential function of Pd1 in the migration of cortical neurons, Pd1-shRNA or control plasmid were transfected into cortical progenitor cells at the VZ by in utero electroporation at E14 or E15. Then the electroporated brains were harvested at E18 or on different postnatal days. At E18, neurons expressing GFP were mainly accumulated at the IZ and only 20% of neurons arrived the CP (Supplementary Fig. S6A, B) in Pd1 suppressed brains. At P0, only

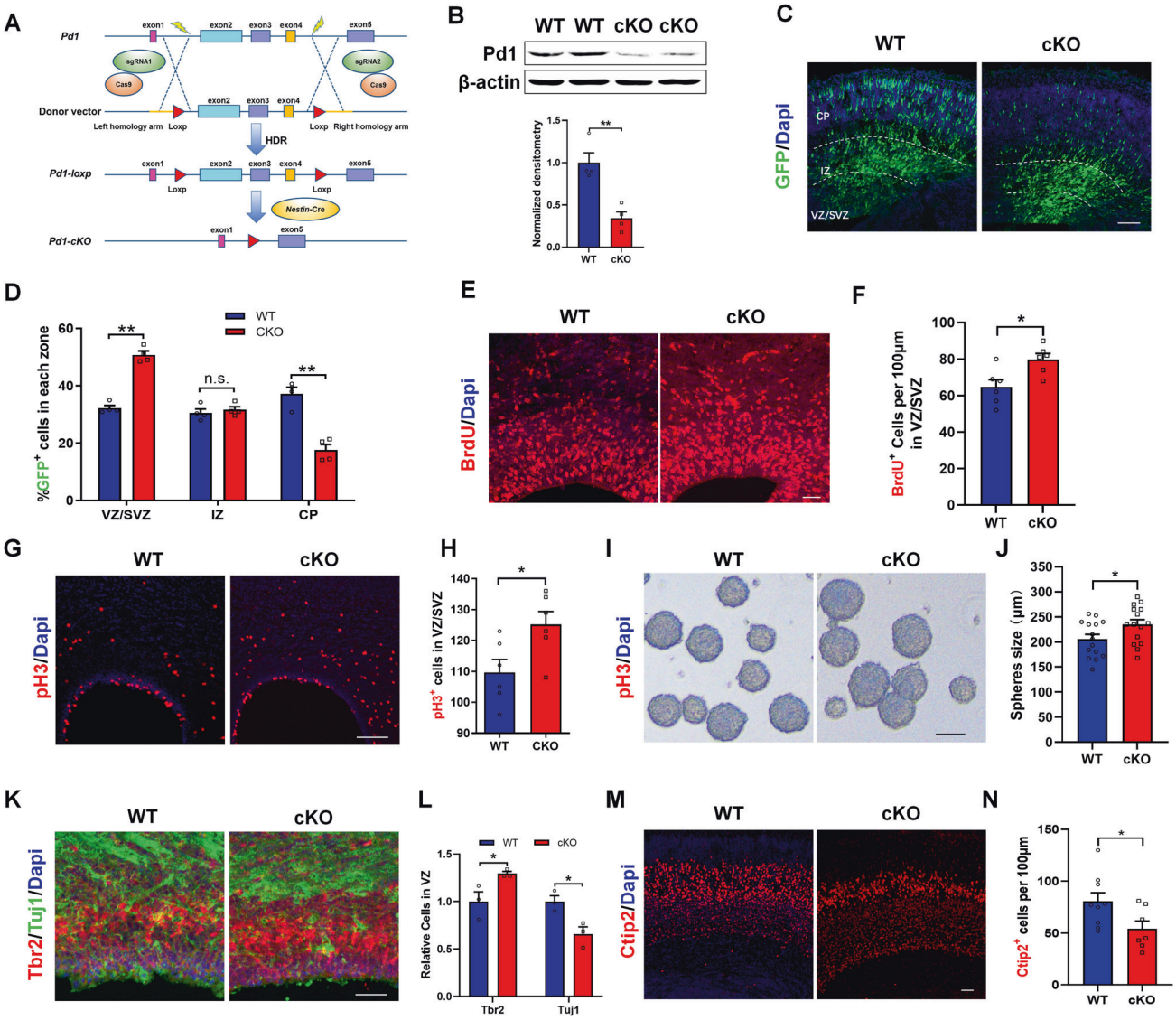

Fig. 2 Pd1 deficiency results in abnormal proliferation and differentiation of neural progenitor cells. A Illustration for the generation of Pd1 knockout mice. To insert two loxP sites into the flank of Pd1 exon2-4, a single long single-stranded oligonucleotide including the homology arms, loxP sites, and Pd1 gene sequence was designed as the donor vector. After cleaving the target DNA by sgRNA and Cas9, the donor vector including loxP sites was introduced into the target gene by homology-directed repair (HDR) to acquire the *Pd1* $^{fl/fl}$ mice. Then the *Pd1* $^{fl/fl}$ mice were crossed with the Nestin-Cre mice to generate *Pd1*^{cKO} mice. **B** Western blot analysis shows that Pd1 is reduced in the brains of *Pd1*^{cKO} mice. *Pd1*$^{fl/fl}$ and *Pd1*^{cKO} are referred to as WT and cKO respectively. $n = 4$ individual experiments and $p = 0.003$. **C** Cell positioning defects are investigated in the cerebral cortex of *Pd1*^{cKO} mice. GFP plasmid was electroporated into the brains of *Pd1*$^{fl/fl}$ and *Pd1*^{cKO} mice at E13. The mice were sacrificed at E16. **D** Graph shows the percentage of GFP$^+$ cells in the VZ/SVZ, IZ, and CP. $n = 5$ mice, $p = 0.00003$ for VZ/SVZ; $p = 0.562$ for IZ; $p = 0.0005$for CP. **E** BrdU incorporation is increased in the sections of *Pd1*^{cKO} mice at E16. The brains of *Pd1*$^{fl/fl}$ or *Pd1*^{cKO} mice were electroporated with a GFP plasmid at E13. BrdU was injected 2 hours before the pregnant mice were sacrificed at E16. **F** The quantification of BrdU$^+$ cells per 100 μm length in VZ/SVZ. $n = 6$ mice and $p = 0.014$. **G** Mitotic index is increased in the brain of *Pd1*^{cKO} mice at E13. **H** Graph shows the number of pH3 positive cells in VZ/SVZ. $n = 6$ mice and $p = 0.026$. **I** Neurospheres generated from *Pd1*^{cKO} mice are larger than those generated from *Pd1*$^{fl/fl}$ mice. NPCs isolated from *Pd1*^{cKO} mice and *Pd1*$^{fl/fl}$ mice were seeded respectively at a low density (200 cells/ml) for culture in proliferation medium for 3 days. **J** Graph shows the statistics of neurosphere diameters. $n = 15$ neurospheres and $p = 0.039$. **K** Coronal brain slices of *Pd1*$^{fl/fl}$ mice and *Pd1*^{cKO} mice at E16 is stained with anti-Tbr2 and anti-Tuj1. **L** Relative numbers of Tbr2$^+$ and Tuj1$^+$ cells in VZ of *Pd1*$^{fl/fl}$ mice and *Pd1*^{cKO} mice. $n = 3$ mice and $p = 0.049$ for Tbr2; $p = 0.025$ for Tuj1. **M** The number of Ctip2$^+$ cells is decreased in *Pd1*^{cKO} mice. **N** Graph shows the number of Ctip2$^+$ cells per 100 μm length. $n = 7$ mice and $p = 0.039$. Error bars represent means ± S.E.M.; Two-tailed unpaired t-test, $P < 0.05$(*), $P < 0.01$(**), n.s., not significant. Scale bars represent 100 μm (**C**, **E**, **G**, **K**, **M**), 200 μm (**I**).

about 40% of labeled cells invaded the CP in Pd1 knockdown brains while almost all labeled cells had arrived at the top layers of CP in control brains (Supplementary Fig. S6C, D). At P7, many labeled cells had arrived at the upper levels of the cortical plate and showed some apical dendrites. Compared with control, there were still some labeled cells that remained ectopic in the WM (Supplementary Fig. S6E, F). At P14, most GFP expressing cells had arrived at the upper layers and displayed highly branched dendrites. Few labeled cells were still impeded in deep cortical layers and the WM (Supplementary Fig. S6G, H). To direct observe the migratory behavior, following the electroporation of GFP plasmid at E13, we performed time-lapse experiments to track the movement of labeled neurons at E14 in cultured brain slices. Compared with control, Pd1 deficient neurons displayed lower levels of migration

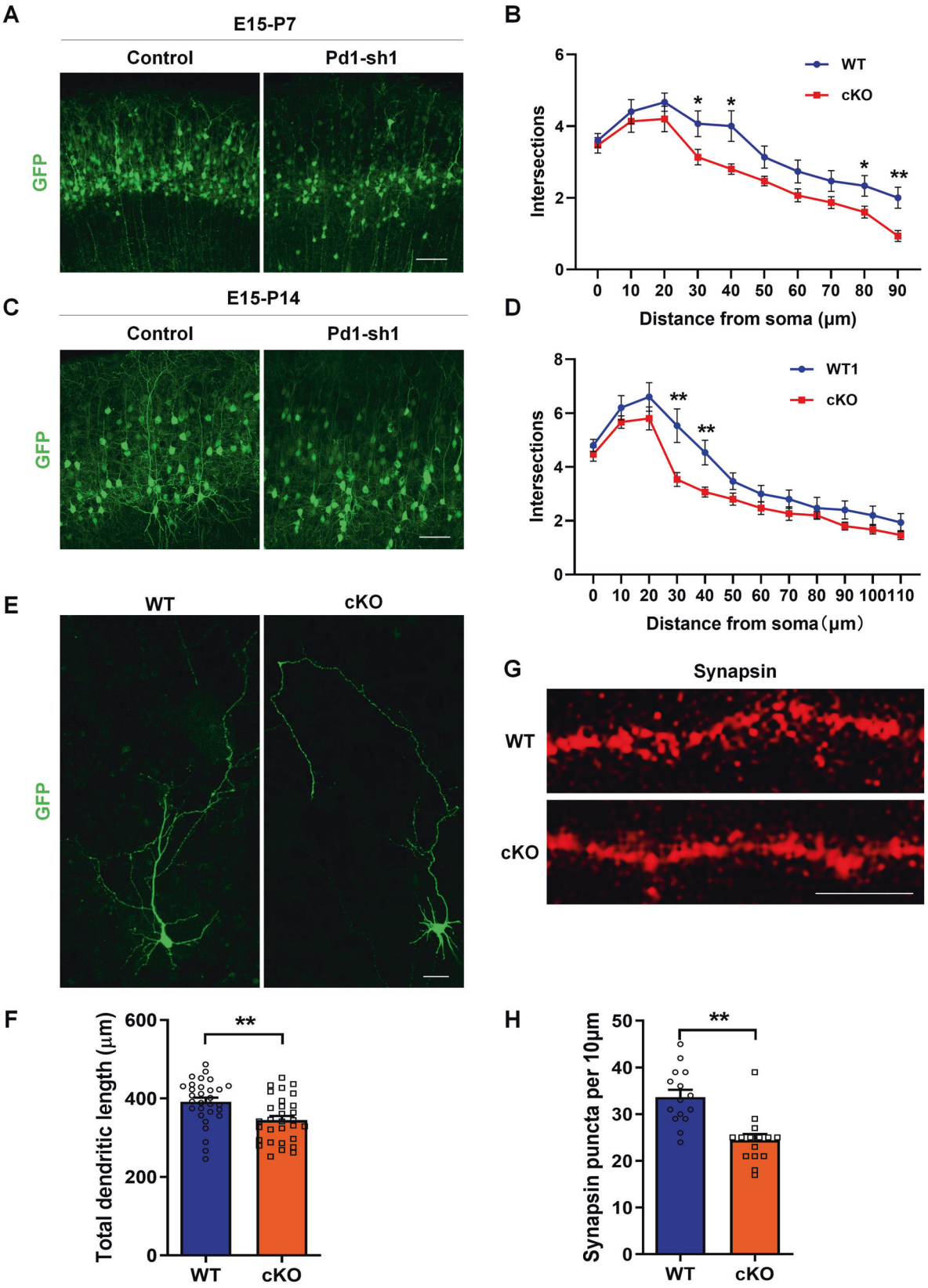

(Supplementary Fig. S6I). Both migration speed and moved distance were decreased upon Pd1 suppression (Supplementary Fig. S6J, K). In all, these results demonstrate that Pd1 is important for the migration of neurons and the final spread in the CP.

Pd1 deficiency results in abnormal neuronal morphology

Since Pd1 perturbs the migration and distribution of neurons, whether Pd1 affects neuronal morphology is unknown. To address this question, Pd1 shRNA and control plasmids were

Fig. 3 Pd1 deficiency results in abnormal neuronal morphology. A Representative images of neurons in the upper layer at P7. Control or Pd1-sh1 plasmid was electroporated at E15 and the brains were harvested at P7. **B** Sholl graphs of dendrites in electroporated neurons at P7 ($n = 15$ cells from 3 animals). **C** Representative images of neurons in the upper layer at P14. Brains were electroporated with control or Pd1-sh1 plasmid at E15 and harvested at P14. **D** Sholl analysis of electroporated neurons at P14 ($n = 15$ cells from 3 animals). **E** Graph shows the morphology of neurons cultured in differentiation medium in vitro. GFP plasmid was electroporated into the brains of $Pd1^{cKO}$ mice and $Pd1^{fl/fl}$ mice at E13 to label the NPCs. At E14, GFP expressed NPCs were selected and cultured in differentiation medium for 6 days. **F** Statistics show that the total dendrites length of neurons is reduced when Pd1 is lost. $n = 30$ cells and $p = 0.003$. **G** Synapsin immunostaining of neurons isolated from WT and cKO mice and cultured in vitro. **H** The number of puncta per 10 μm dendrite. $n = 15$ and $p = 0.00009$. Error bars represent means ± S.E.M.; Two-tailed unpaired t-test, $P < 0.05$(*), $P < 0.01$(**), n.s. not significant. The scale bar represents 100 μm (**A**, **C**), 20 μm (**E**), and 10 μm (**G**).

electroporated at E15 respectively. Neuron morphology was investigated at P7 or P14. When Pd1 was depressed, neurons that migrated to the CP displayed abnormal neuronal morphology at P7. Not only the total length of dendrites but also the number of branching was reduced (Fig. 3A, B). At P14, a dramatic reduction in dendritic length and branching number in Pd1 suppressed neurons was still investigated (Fig. 3C, D). To observe the morphology of individual isolated neurons, we electroporated GFP plasmid into the brains of $Pd1^{fl/fl}$ and $Pd1^{cKO}$ mice at E13 and isolated neural progenitor cells from GFP-labeled brains at E14. After 6 days culture in differentiated medium, the morphology of GFP-positive neurons was collected. Neurons isolated from $Pd1^{cKO}$ mice also exhibited abnormal morphology. The total dendritic length was reduced in *Pd1*-deleted neurons (Fig. 3E, F). To analyze the effect of Pd1 on synapse formation, we performed synapsin immunostaining on primary cultured cortical neurons. Compared with $Pd1^{fl/fl}$, the density of synapse puncta on dendrites was decreased in neurons isolated from $Pd1^{cKO}$ mice brains (Fig. 3G, H). Altogether, these results demonstrate that Pd1 is necessary for dendritic growth and morphology formation.

Pd1 deletion elicits behavioral deficits

The defects in embryonic neurogenesis caused by Pd1 loss or depression promote us to explore the behavioral consequences of $Pd1^{cKO}$ mice. For this purpose, $Pd1^{cKO}$ mice and their littermate $Pd1^{fl/fl}$ mice at approximately 8-12 weeks of age were first subject to the open field test. The time spent in the center was decreased in $Pd1^{cKO}$ mice (Fig. 4A, Supplementary Fig. S7A), although the total traveled distance had no significant difference between $Pd1^{fl/fl}$ mice and $Pd1^{cKO}$ mice (Supplementary Fig. S7B). These results indicate that the exploratory activity of $Pd1^{cKO}$ mice was reduced and the general locomotion was not affected. Next, an elevated-plus maze was employed to detect anxiety-like behavior. Compared with $pd1^{fl/fl}$ mice, $Pd1^{cKO}$ mice were prone to stay in the closed arms (Fig. 4B, Supplementary Fig. S7C) and spent less time in the open arms (Fig. 4C, Supplementary Fig. S7C), exhibiting a certain amount of anxiety. The traveled distance of mice in elevated-plus was also no significant difference (Supplementary Fig. S7D). Y maze test showed the working memory is impaired in $Pd1^{cKO}$ mice as the spontaneous alternation was reduced (Fig. 4D). To assess potential depressive-like behaviors, $Pd1^{cKO}$ mice and their littermate $Pd1^{fl/fl}$ mice were used in forced swimming tests (FSTs), tail suspension tests (TSTs), and sucrose preference tests (SPTs). The latency time to immobility decreased (Fig. 4E) and the immobility duration increased (Fig. 4F) in $Pd1^{cKO}$ mice. In TSTs, $Pd1^{cKO}$ mice showed a significant increase in the immobility time (Fig. 4G), suggesting a despair behavior under pressure. SPTs showed that the anhedonia was popular in $Pd1^{cKO}$ mice as the sucrose consumption was reduced (Fig. 4H). Furthermore, social interactivity was detected by three-chamber social arena assays. Compared with $Pd1^{fl/fl}$ mice, $Pd1^{cKO}$ mice had no marked preference to interact with the novel mice, demonstrating that the social interactivity was impaired when *Pd1* was deleted in mice (Fig. 4I, J). In addition, the time spent sniffing the cylinder containing the novel mice, as well as the time spent near the cylinder were not obviously different in $Pd1^{cKO}$ mice (Supplementary Fig. S7E, F). Consistently, no difference was observed in rotarod tests and grip strength tests, indicating that the loss of Pd1 has no marked effect on motor coordination and function (Supplementary Fig. S7G, H). Taken together, $Pd1^{cKO}$ mice exhibit depressive-like behaviors, including anxiety, despair, anhedonia, and deficits in exploratory activity, working memory, or social interactivity.

Pd1 regulates brain development by targeting Pax3

To shed light on the molecular mechanisms associated with the regulation of Pd1 on embryonic cortical development, the mRNA expression profiles were analyzed in the brains isolated from $Pd1^{fl/fl}$ mice and $Pd1^{cKO}$ mice at E13 by RNA-seq. A genome-wide change was investigated when Pd1 was lost (Fig. 5A). Go biological process analysis revealed that the regulated gene was mainly enriched in the development of the central nervous system, generation of neurons, and neuron differentiation (Fig. 5B). To identify the target of Pd1 downstream, we do volcano plot. Among the up-regulated genes, Pax3 was altered significantly in the RNA-seq (Fig. 5C). To further verify the result, we detected the expression of Pax3 by RT-PCR. When Pd1 was down-regulated, the mRNA level of Pax3 was significantly up-regulated compared with Tlx3 and Dgkg, which is also up-regulated in RNA-seq (Fig. 5D, E). When Pax3 was down-regulated, electroporated brains exhibited cell positioning defects. Fewer GFP^+ cells in the VZ/SVZ and more GFP^+ cells in the CP, which was in contrast to the phenotype of Pd1 knockdown (Fig. 5F, G). Simultaneously, the mitotic activity (Supplementary Fig. S8A, B) and BrdU incorporation (Supplementary Fig. S8C, D) were decreased. Meanwhile, the neurons labeled by Tuj1 were increased (Supplementary Fig. S8E, F). These results indicate that Pax3 plays an essential role in embryonic neurogenesis. To illustrate the regulation of Pd1 on embryonic brain development was carried out through Pax3, rescue experiments were performed. Not only the abnormal cell distribution but also the proliferative and differential defects caused by Pd1 knockdown could be partially rescued by the decreased Pax3 levels (Fig. 5H–M). These results suggest that Pax3 is a downstream effector of Pd1 regulating embryonic neurogenesis.

Pd1 regulates the expression of Pax3 via AKT/GSK3β/β-catenin signaling pathway

To further decipher the relationship between Pd1 and Pax3, a set of signaling pathways was analyzed by western blotting. We found AKT/GSK3β/β-catenin signaling pathway was involved in the regulation of Pd1 on Pax3. When Pd1 was deleted, the level of p-AKT/ P-GSK3β(S9)/β-catenin was increased while the level of P-GSK3β(Y216)/p-β-catenin was decreased (Fig. 6A). When Pd1 was down-regulated, the level of β-catenin was also increased (Fig. 6B). Consistently, the level of β-catenin was decreased when Pd1 was overexpressed. The reduction of β-catenin was more obvious when both of Pd1 and PdL1 were overexpressed (Fig. 6C). The addition of XAV939 into the medium not only significantly decreased the level of β-catenin but also reduced the expression of Pax3 (Fig. 6D). In addition, the proliferative marker pH3 was decreased and neuronal marker Tuj1 was increased, which was consisted with the phenotype of β-catenin knockdown (Fig. 6D). To detect the regulation of Pd1 on AKT/GSK3β/β-catenin signaling pathway is mediated by SHP2, the

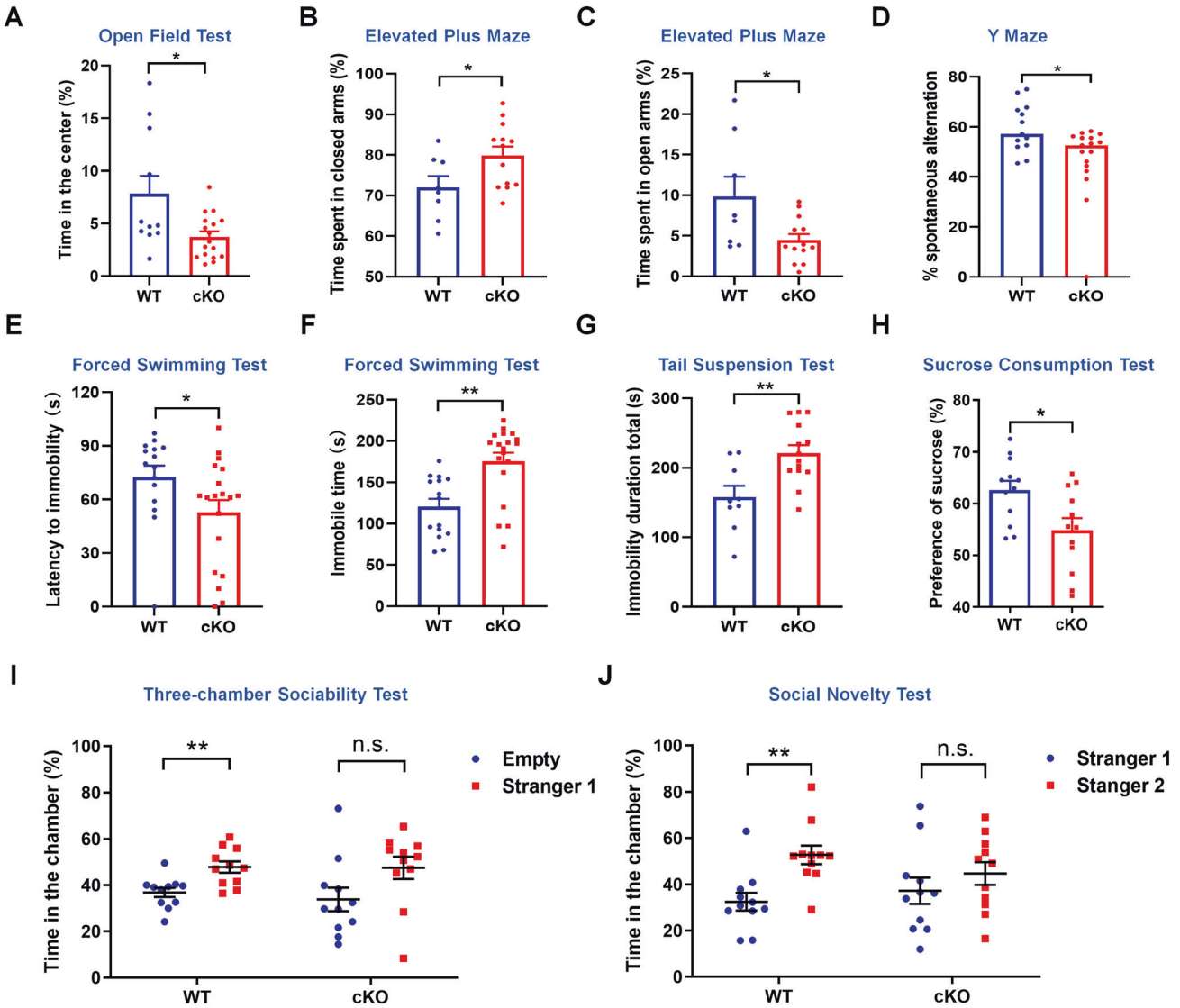

Fig. 4 ***Pd1* deletion leads to depressive-like behaviors in mice. A** Graph shows $Pd1^{cKO}$ mice spent less time in the center than $Pd1^{fl/fl}$ mice in the open field test. $n = 11$ for $Pd1^{fl/fl}$ mice, $n = 17$ for $Pd1^{cKO}$ mice, and $p = 0.011$. **B** Compared with $Pd1^{fl/fl}$ mice, $Pd1^{cKO}$ mice spent more time in the closed arms in the elevated plus maze test. $n = 8$ for $Pd1^{fl/fl}$ mice, $n = 13$ for $Pd1^{cKO}$ mice, and $p = 0.038$. **C** Compared with $Pd1^{fl/fl}$ mice, $Pd1^{cKO}$ mice spent less time in the open arms in the elevated plus maze test. $n = 8$ for $Pd1^{fl/fl}$ mice, $n = 13$ for $Pd1^{cKO}$ mice, and $p = 0.021$. **D** The percentage of spontaneous alternation in $Pd1^{cKO}$ mice is reduced. $n = 13$ for $Pd1^{fl/fl}$ mice, $n = 17$ for $Pd1^{cKO}$ mice, and $p = 0.013$. **E** The latency to immobility of $Pd1^{cKO}$ mice is reduced compared with $Pd1^{fl/fl}$ mice in FST. $n = 15$ for $Pd1^{fl/fl}$ mice, $n = 19$ for $Pd1^{cKO}$ mice, and $p = 0.047$. **F** The immobile time of $Pd1^{cKO}$ mice is longer than that of $Pd1^{fl/fl}$ mice in FST. $n = 15$ for $Pd1^{fl/fl}$ mice, $n = 19$ for $Pd1^{cKO}$ mice, and $p = 0.0006$. **G** The total immobile time of $Pd1^{cKO}$ mice is significantly prolonged in TST. $n = 9$ for $Pd1^{fl/fl}$ mice, $n = 14$ for $Pd1^{cKO}$ mice, and $p = 0.004$. **H** Sucrose preference test shows the sucrose consumption of $Pd1^{cKO}$ mice is less than that of $Pd1^{fl/fl}$ mice in SPT. $n = 12$ for $Pd1^{fl/fl}$ mice, $n = 12$ for $Pd1^{cKO}$ mice, and $p = 0.015$. **I** Compared with $Pd1^{fl/fl}$ mice, $Pd1^{cKO}$ mice have no obvious social preference with stranger1 mouse. $Pd1^{fl/fl}$ mice spend more time in the chamber with stranger1 than in the empty chamber. $n = 11$ for $Pd1^{fl/fl}$ mice, and $p = 0.003$; $n = 11$ for $Pd1^{cKO}$ mice, and $p = 0.067$. **J** $Pd1^{cKO}$ mice have not prone to socializing with stranger2 mice, as the time spent in the chamber with a new unfamiliar mouse (stranger2) and in the opposite chamber with a familiar mouse (stranger2) has no significant difference. $n = 11$ for $Pd1^{fl/fl}$ mice, and $p = 0.002$; $n = 11$ for $Pd1^{cKO}$ mice, and $p = 0.332$. Error bars represent means ± S.E.M.; Two-tailed unpaired t-test, $P < 0.05$(*), $P < 0.01$(**), n.s. not significant.

inhibitor of SHP2 (SHP099) was added into the medium of NSCs. Compared with the control and Pd1 downregulated group, the increase of p-AKT and β-catenin were more obvious, indicating SHP2 is an essential mediator (Fig. 6E). To test whether the reduced β-catenin mediated by XAV939 can rescue the deficient of brain development caused by Pd1 knockdown, Pd1-shRNA and control plasmids were electroporated into the embryonic brains respectively. Then the XAV939 and DMSO were intraperitoneally injected into the pregnant mice once a day from E14 to E16. Compared with DMSO treatment, the administration of XAV939 could partially rescue the deficiency of brain development caused by Pd1 down-regulation (Fig. 6F, G). The previous reports showed that the promoter of Pax3 is active by the β-catenin signaling pathway [13]. To verify the binding of β-catenin on the Pax3 promoter, chromatin immunoprecipitation was performed. The results showed that β-catenin binds to the 1 kb upstream of the transcriptional start site of the Pax3 promoter (Fig. 6H). Together, these results indicate that Pd1 regulates the expression of Pax3 through AKT/GSK3β/β-catenin signaling pathway (Fig. 6I).

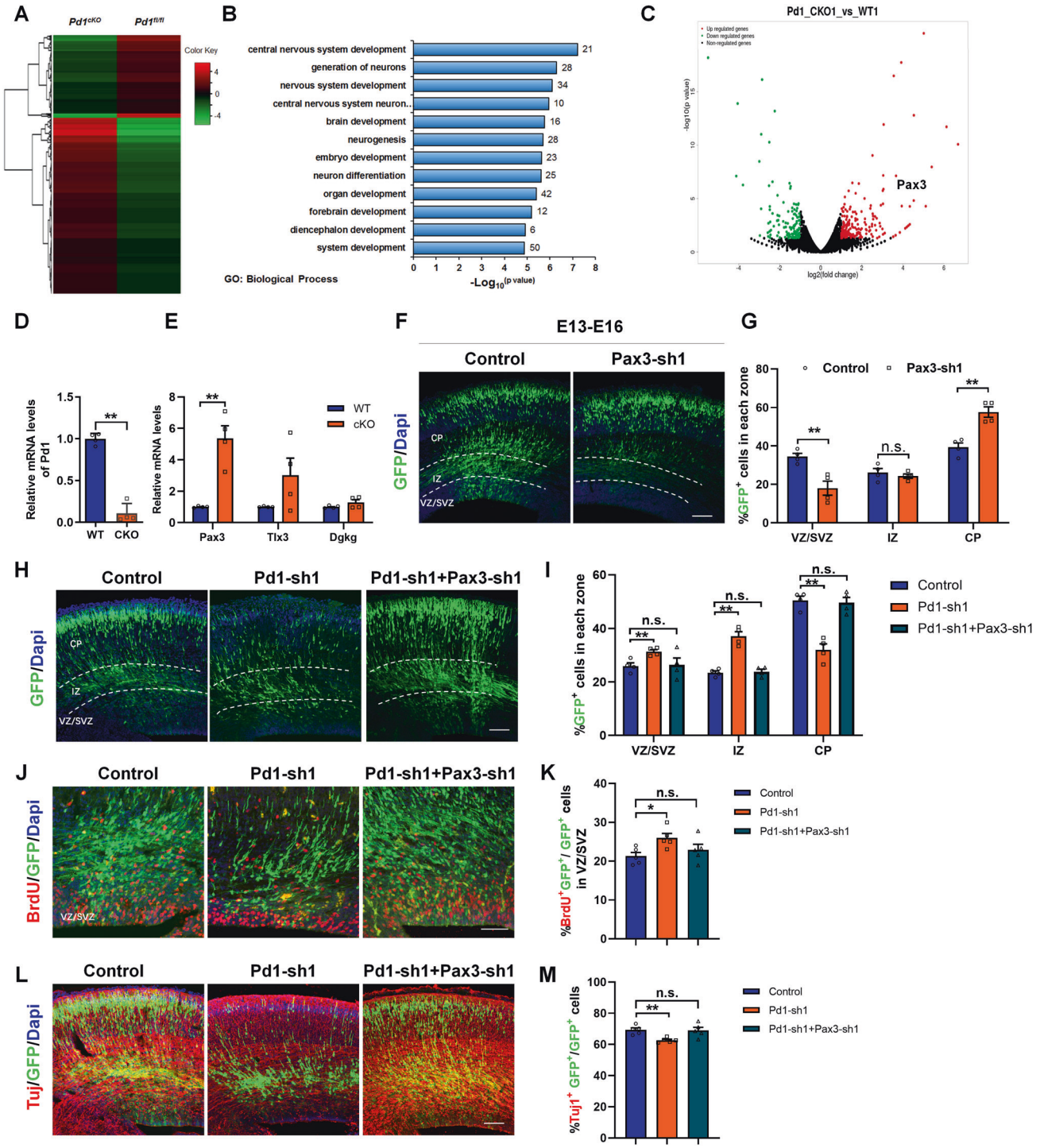

XAV939 treatment ameliorate behaviors defect in *Pd1*^{cKO} mice

Previous reports showed that XAV939 has an antidepressant effect in adult mice by promoting hippocampal neurogenesis (Chen et al., 2019). To determine whether XAV939 can rescue depressive-like behaviors in *Pd1*^{cKO} mice, pregnant mice were administered XAV939 by intraperitoneal injection once a day from E13 until *Pd1*^{cKO} mice and *Pd1*$^{fl/fl}$ mice were born (Fig. 7A). The behavior test was carried out on the sixth week after birth. FST experiments showed the administration of XAV939 significantly decrease the immobility and increase the latency to immobility in *Pd1*^{cKO} mice (Fig. 7B, C). In TSTs, XAV939 treatment also reduced the despair of *Pd1*^{cKO} mice (Fig. 7D). The preference for sucrose was no significant difference between *Pd1*^{cKO} mice and *Pd1*$^{fl/fl}$ mice after XAV939 administration (Fig. 7E), indicating anhedonia in *Pd1*^{cKO} mice can be rescued. The social interaction deficits were ameliorated as the contact with novel mice was enhanced (Fig. 7F, G). In addition, the exploratory behavior of *Pd1*^{cKO} mice was increased in the open field test (Fig. 7H). Meanwhile, DMSO treatment has no effects on the depressive-like behaviors of *Pd1*^{cKO} mice in all the behavior tests. These results suggest that XAV939 treatment ameliorates the depressive-like behavior deficits in *Pd1*^{cKO} mice.

Fig. 5 Pd1 regulates embryonic neurogenesis by targeting Pax3. A Pd1 deletion results in global gene expression variation. Hierarchical clustering analysis of genes that change fold is more than two between $Pd1^{fl/fl}$ mice and $Pd1^{cKO}$ mice. **B** Gene ontology analysis of dysregulated genes in $Pd1^{cKO}$ mice brains. **C** Image of Volcano plots shows the downregulated (green) and upregulated genes (red). **D** The mRNA level of Pd1 is obviously reduced upon *Pd1* deletion. $n = 4$ individual experiments and $p = 0.00001$. **E** Loss of *Pd1* results in an obvious increase in the expression of Pax3. $n = 4$ individual experiments and $p = 0.002$ for Pax3; $p = 0.116$ for Tlx3; $p = 0.172$ for Dgkg. **F** Downregulation of Pax3 leads to abnormal cell distribution in brain development. The plasmid of control and Pax3-sh1 were electroporated into the embryonic brain respectively at E13 and collected at E16 for further analysis. **G** Percentage of GFP^+ cells in each zone of the cerebral cortex. $n = 4$ mice, $p = 0.007$ for VZ/SVZ; $p = 0.468$ for IZ; $p = 0.002$ for CP. **H** Abnormal cell distribution caused by Pd1 downregulation is partially rescued by Pax3-shRNA. **I** Graph shows the percentage of GFP^+ cells in each zone. $p = 4$ mice, $p = 0.009$ (Control&Pd1-sh1) and $p = 0.889$ (Control&Pd1-sh1+Pax3-sh1) for VZ/SVZ; $p = 0.0003$ (Control&Pd1-sh1) and $p = 0.726$ (Control&Pd1-sh1+Pax3-sh1) for IZ; $p = 0.0005$ (Control&Pd1-sh1) and $p = 0.753$ (Control&Pd1-sh1+Pax3-sh1) for CP. **J** BrdU incorporation defects induced by Pd1 knockdown are rescued by Pax3 suppression. **K** Graph shows the percentage of BrdU incorporation in GFP^+ cells in VZ/SVZ. $n = 5$ mice, $p = 0.014$ for Control&Pd1-sh1; $p = 0.383$ for Control&Pd1-sh1+Pax3-sh1. **L** Downregulation of Pax3 overrides neuronal differentiation defects caused by Pd1 knockdown. **M** Graph shows the percentage of $Tuj1^+GFP^+$ cells relative to all GFP^+ cells. $n = 5$ mice, $p = 0.002$ for Control&Pd1-sh1; $p = 0.884$ for Control&Pd1-sh1+Pax3-sh1. Error bars represent means ± S.E.M.; Two-tailed unpaired t-test, $P < 0.05$(*), $P < 0.01$(**), n.s. not significant. The scale bar represents 100 μm.

PD1 directs the proliferation and differentiation of human NPCs (hNPCs)

It is generally believed that Pd1 is an inhibitory immune molecule, but less is known about the expression and function in hNPCs proliferation and differentiation. Immunostaining showed that Pd1 is expressed in human neural progenitor cells (Supplementary Fig. S9A) and co-labeled with NESTIN (Supplementary Fig. S9B). When PD1 was inhibited by shRNA, the numbers of $NESTIN^+GFP^+$ were increased in lentivirus-infected cells (Supplementary Fig. S9C, D). Meanwhile, the number of $TUJ1^+GFP^+$ cells was reduced (Supplementary Fig. S9E, F). These results indicate that PD1 also plays an essential role in the proliferation and differentiation of hNPCs.

DISCUSSION

Pd1, a trans-membrane protein, is well-known in the immune system for its essential roles in inhibiting immune responses as well as promoting self-tolerance [14]. Accumulating evidence shows that many proteins discovered in the immune system are also expressed in the nervous system and play different functions in the brain [15]. Whether Pd1 has more than one role in different tissues or cell types is unknown. In this study, we found Pd1 is expressed in the embryonic brain including NSCs and neurons. The disturbance of Pd1 results in abnormal cell distribution and deficiency in neurogenesis. Not only the differentiation and migration but also the morphology of neurons is disrupted when Pd1 is down-regulated. During the behavior tests, $Pd1^{cKO}$ mice are prone to be depressed, including despair, anhedonia, and social withdrawal. The regulation of Pd1 on brain development is mediated by Pax3 through AKT/GSK-3β/β-catenin signaling pathway. The downregulation of Pax3 or XAV939 treatment can partially rescue the deficiency in embryonic neurogenesis caused by Pd1 depletion. Simultaneously, the abnormal behavior of $Pd1^{cKO}$ mice can be ameliorated by XAV939 administration. Our results illustrate novel, nonimmune functions of Pd1 in the development of brain, shedding a new light on the physiological and pathological significance of immune protein in brain development.

Major depressive disorder is one common mental disease and is prevalent worldwide. The pathogenesis of MDD remains largely unknown. Multiple factors contribute to the occurrence of MDD, such as the deficiency of neurotrophic factors [16], the dysfunction of the immune system [17], and the alterations in the gut microbiota populations [18]. Neuroimaging detection exhibit alternation in cortical thickness in patients diagnosed with MDD [19]. Whether such alternations are caused by the impairments of embryonic neurogenesis and what are the pathologies mechanisms involved in MDD remains largely unknown. Although abnormal cortical development and deficiency in neurogenesis were related to MDD [20, 21], the mechanisms underlying MDD, especially the potential relationship between brain development and MDD is not well illustrated. In this study, the loss of Pd1 may disturb the balance between progenitor proliferation and differentiation, affect the migration and integration of newly born neurons, and finally result in the predisposition of MDD (Supplementary Fig. S10).

In this study, we found the regulation of Pd1 in embryonic neurogenesis is mainly mediated by β-catenin. Previous reports showed that β-catenin has been involved in major depressive disorder. The increase of β-catenin caused by antagomir-214-3p can reverse the depressive-like behavior in CSDS mice [22]. Compared with non-depressed subjects, the level of β-catenin decreased in the prefrontal cortex of MDD [23]. In β-catenin KO mice, the immobility time is significantly increased in TST, exhibiting abnormal behavior relevant to depression [24]. In transgenic mice that overexpress β-catenin, the immobility time in FST decreased, demonstrating a potential therapeutic strategy for related disease [16]. Most studies focus on the function of β-catenin in adult MDD individuals. Whether the role of β-catenin in brain development is related to MDD is rarely studied. Enhancing the stabilization of β-catenin increases the number of proliferative precursors and results in an enlarged brain [25]. Conditional inactivation of β-catenin results in failed development of the cortex, including decreased cell proliferation, increased neuronal differentiation, and impaired neuronal migration [26]. Consistently, down-regulation of β-catenin causes abnormal cell distribution in the cerebral cortex. The number of GFP-positive cells is increased in CP and is reduced in VZ/SVZ when β-catenin is suppressed [27]. Although the function of β-catenin in brain development is clearly described, whether the dysregulation of β-catenin contributes to the onset of MDD is unknown. XAV939 is a small molecule which stimulates β-catenin degradation by stabilizing Axin. The injection of XAV939 not only partially rescues the abnormal distribution caused by Pd1 downregulated but also ameliorate the depression-like behaviors in mice, indicating that the β-catenin signaling pathway plays an essential role in the brain development and the onset of MDD.

Pd1 involves entire embryonic neurogenesis. Not only the proliferation and differentiation of NPCs but also the migration of newly born neurons is regulated by Pd1 during brain development. When Pd1 is downregulated, the migration of neurons is delayed. Although the migration delay is not lead to obvious structural defects, it may result in abnormal connections between neurons, as well as the integration of neurons into cortical circuits during brain development. In addition, abnormal morphology is observed in Pd1 suppressed neurons. The improper synapse formation may also cause impairments of functional connectivity between neurons. Whether the abnormal neurogenesis and impaired connectivity of neurons is the major cause of MDD needs further exploration. Previous reports showed that one obvious characteristic of MDD patients is the reduction of hippocampus volume [28–30]. Two hypotheses have been proposed to explain this phenotype: one is decreased

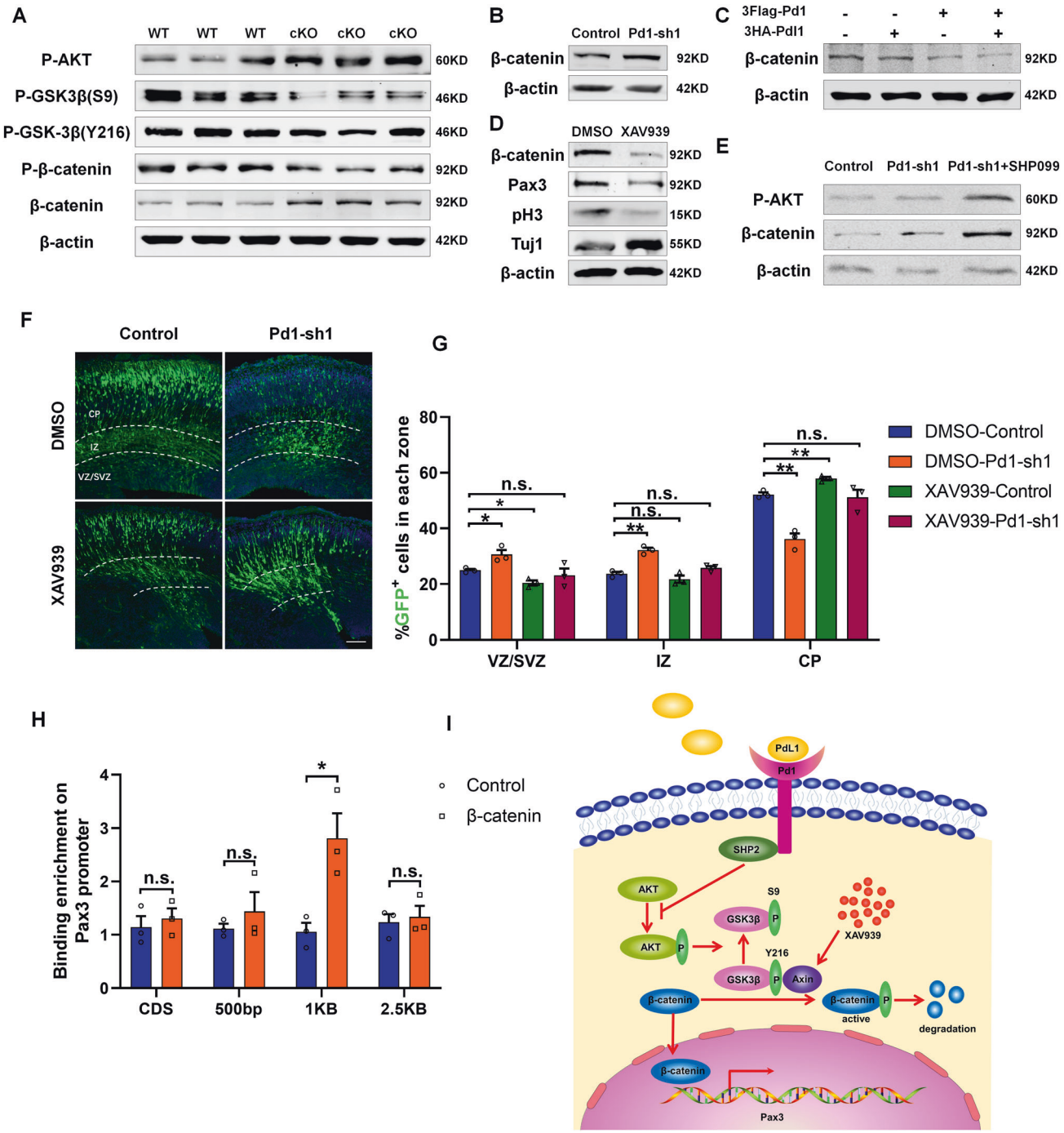

Fig. 6 Pd1 regulates Pax3 expression through AKT/GSK-3β/β-catenin signaling pathway. A Western blot analysis shows that Pd1 mediates the activation of the AKT/GSK-3β/β-catenin signaling pathway in brains. Proteins extracted from the brains of WT and cKO mice were probed with anti-p-AKT, anti-p-GSK3β(S9), anti-p-GSK3β(Y216), anti-p-β-catenin, anti-β-catenin, and anti-β-actin antibodies. **B** The level of β-catenin is increased when Pd1 is downregulated by shRNA. **C** The level of β-catenin is decreased obviously when both Pd1 and Pdl1 are overexpressed. **D** The level of β-catenin and Pax3 is reduced when XAV939 is added into the medium of NPCs. **E** The regulation of Pd1 on the AKT/GSK-3β/β-catenin pathway is mediated by SHP2. NPCs cultured in 6 well plates were infected with control and Pd1-sh1 lentivirus. Two days later, NPCs were treated with SHP099 at a concentration of 20 μM for 2 h at 37 °C and then harvested for the western blotting experiment. **F** Abnormal cell distribution caused by Pd1 suppression is rescued by the XAV939 administration. **G** Graph shows the percentage of GFP^+ cells in each zone. $n = 3$ mice, $p = 0.029$ (DMSO-Control & DMSO-Pd1-sh1), $p = 0.01$ (DMSO-Control &XAV939-Control), $p = 0.508$ (XAV939-Control&XAV939-Pd1-sh1) for VZ/SVZ; $p = 0.001$ (DMSO-Control & DMSO-Pd1-sh1), $p = 0.243$ (DMSO-Control &XAV939-Control), $p = 0.106$ (XAV939-Control&XAV939-Pd1-sh1) for IZ; $p = 0.002$ (DMSO-Control & DMSO-Pd1-sh1), $p = 0.005$ (DMSO-Control &XAV939-Control), $p = 0.732$ (XAV939-Control&XAV939-Pd1-sh1) for CP. **H** Binding enrichment analysis of β-catenin on Pax3 promoter. The primary NSCs infected with lentivirus expressing β-catenin were subjected to chromatin immunoprecipitation experiments. $n = 3$ individual experiments, $p = 0.59$ for CDS; $p = 0.436$ for 500 bp; $p = 0.024$ for 1 kb; $p = 0.713$ for 2.5 kb. **I** Summary of Pd1 regulation on Pax3 via AKT/GSK-3β/β-catenin signaling pathway. Error bars represent means ± S.E.M.; Two-tailed unpaired t-test, $P < 0.05$(*), $P < 0.01$(**), n.s. not significant. The scale bar represents 100 μm.

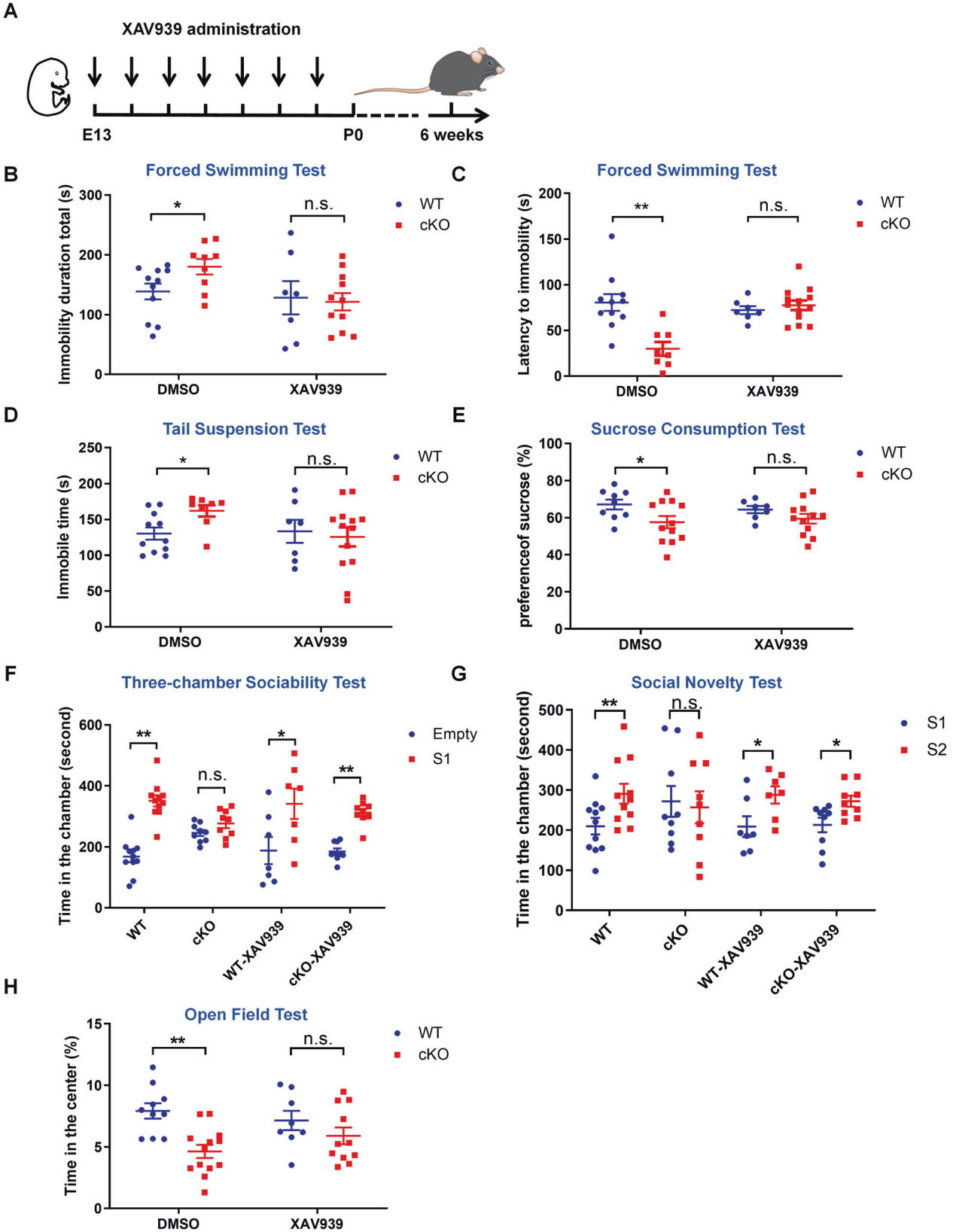

neurogenesis and the other is neuroplasticity which is accompanied by morphological changes including shortened dendrites [1]. Our findings supported these hypotheses, but more studies are needed to draw more definitive conclusions. In addition, our results suggest that Pd1 may be predictive of neurodevelopmental disorders as it's essential role in embryonic neurogenesis, but the linkage between Pd1 and human brain disease needs to be further studied.

Fig. 7 XAV939 administration ameliorates the abnormal behaviors in $Pd1^{cKO}$ mice. A Illustration of XAV939 administration in embryonic mice. E13 $Pd1^{cKO}$ and littermate mice $Pd1^{fl/fl}$ mice were treated with XAV939 or DMSO until they were born. Six weeks later, the mice were subjected to behavioral analysis. **B** The immobile time of mice in the forced swimming test (DMSO group, $n = 11$ for $Pd1^{fl/fl}$ mice, $n = 9$ for $Pd1^{cKO}$ mice, and $p = 0.041$; XAV939 group, $n = 7$ for $Pd1^{fl/fl}$ mice, $n = 11$ for $Pd1^{cKO}$ mice, and $p = 0.882$). **C** Latency to immobility of mice in the forced swimming test (DMSO group, $n = 11$ for $Pd1^{fl/fl}$ mice, $n = 8$ for $pd1^{cKO}$ mice, and $p = 0.0009$; XAV939 group, $n = 7$ for $Pd1^{fl/fl}$ mice, $n = 13$ for $Pd1^{cKO}$ mice, and $p = 0.502$). **D** The total immobile time of mice in the tail suspension test (DMSO group, $n = 11$ for $Pd1^{fl/fl}$ mice, $n = 8$ for $Pd1^{cKO}$ mice, and $p = 0.017$; XAV939 group, $n = 7$ for $Pd1^{fl/fl}$ mice, $n = 13$ for $Pd1^{cKO}$ mice, and $p = 0.725$). **E** The sucrose consumption of mice in the sucrose preference test (DMSO group, $n = 9$ for $Pd1^{fl/fl}$ mice, $n = 12$ for $Pd1^{cKO}$ mice, $p = 0.044$; XAV939 group, $n = 7$ for $Pd1^{fl/fl}$ mice, $n = 12$ for $Pd1^{cKO}$ mice, and $p = 0.206$). **F** Statistic of the time that mice spend in the chambers with empty cylinder or with stranger mice 1 respectively (DMSO group, $n = 11$ for $Pd1^{fl/fl}$ mice, $p = 0.0002$; $n = 9$ for $Pd1^{cKO}$ mice, $p = 0.108$; XAV939 group, $n = 7$ for $Pd1^{fl/fl}$ mice, $p = 0.041$; $n = 9$ for $Pd1^{cKO}$ mice, and $p = 0.0007$). **G** Statistic of the time that mice spend in the chambers with stranger mice 1 or with stranger mice 2 respectively (DMSO group, $n = 11$ for $Pd1^{fl/fl}$ mice, $p = 0.007$; $n = 9$ for $Pd1^{cKO}$ mice, $p = 0.792$; XAV939 group, $n = 7$ for $Pd1^{fl/fl}$ mice, $p = 0.036$; $n = 9$ for $Pd1^{cKO}$ mice, and $p = 0.018$). **H** Time in the center in open field test (DMSO group, $n = 10$ for $Pd1^{fl/fl}$ mice, $n = 13$ for $Pd1^{cKO}$ mice, $p = 0.0006$; XAV939 group, $n = 8$ for $Pd1^{fl/fl}$ mice, $n = 11$ for $Pd1^{cKO}$ mice, and $p = 0.248$). Error bars represent means ± S.E.M.; one-way ANOVA, $P < 0.05$ (*), $P < 0.01$(**), and n.s. not significant.

PD1 play diverse functions in both physiological and pathological conditions. PD1 not only is a major immunotherapy target in tumor treatment but also involves multiple CNS disorders such as pain [10] and cognitive function [11]. PD1 play functions in the CNS either through resident microglia and other peripheral immune cells or by its endogenous expression in neuronal cells [31]. Recently, the regulation of neuronal Pd1 in learning and memory is addressed. When *Pd1* is globally knocked out or selectively deleted in excitatory neurons, the cognitive function of mice is promoted [32]. Our data showed that the specific deletion of Pd1 in NPCs results in abnormal brain development and depressive-like behaviors. The dysfunction of Pd1 in the early development of the brain cascades onto a broad array of subsequent cellular processes and exerts a long-lasting effect on brain function which are not easily be compensated. There results indicate the diverse functions of Pd1 in different cells and different developmental stages. To full understanding the function of PD-1 in the cross-talk between NSCs, neurons, microglial, and peripheral immune cells, more studies are needed, which will shed light on immunomodulation and novel strategies for treating brain diseases.

MATERIALS AND METHODS

Generation of $Pd1^{fl/fl}$ mice

$Pd1^{fl/fl}$ mice were generated by CRISPR-Cas9 HDR system in the Experimental Animal Center of the Institute of Zoology, Chinese Academy of Sciences. Briefly, Double-Stranded Breaks flanking exon 2 and exon 4 were generated by using CRISPR and sgRNA. Then the purified sg RNA, Cas9 mRNA, and donor DNA (loxP-exon2,3,4- loxp flanked with 5′homologous arm/3′homologous arm) were microinjected into fertilized single-cell embryos. The $Pd1^{fl/+}$ mice (F0) were generated by Homology Directed Repair (HDR). F0 mice were confirmed by tail genotyping and PCR production sequencing. After breeding, $Pd1^{fl/fl}$ mice were acquired and crossed with the Nestin-Cre mice to generate $Pd1^{cKO}$ mice.

Animals

All animal experiments were performed following the guidelines for the care and use of laboratory animals and were approved by the Institutional Animal Care and Use Committee of the Institute of Zoology, Chinese Academy of Sciences. $Pd1^{fl/fl}$ mice were generated by the Experimental Animal Center of the Institute of Zoology and crossed with Nestin-cre mice. The Institute of Cancer Research (ICR) pregnant mice used for in utero electroporation or NPCs isolation were purchased from Vital River Laboratories or SPF (Beijing) Biotechnology Co., Ltd. All mice were housed at a proper room temperature with a 12/12 light-dark cycle.

Time lapse of electroporated brain slice

Embryonic brains were electroporated at E13 and collected at E15. Embryonic brain slices with 300 um thickness were prepared by using a Leica VT1000S vibrosector. Slices were cultured in a μ-Slide 8 well (ibidi) with NSC proliferation medium. Time-lapse confocal microscopy was performed using PerkinElmer UltraVIEW-VoX. Images were acquired at preselected positions with multiple z stacks on the electroporated brain slices. Acquisitions were repeated every 40 min for up to 6 h.

DATA AVAILABILITY

RNA-seq data are available in GEO with the following accession number: GSE207712.

REFERENCES

1. Boku S, Nakagawa S, Toda H, Hishimoto A. Neural basis of major depressive disorder: beyond monoamine hypothesis. Psychiatry Clin Neurosci. 2018;72:3–12.
2. Barch DM, Tillman R, Kelly D, Whalen D, Gilbert K, Luby JL. Hippocampal volume and depression among young children. Psychiatry Res Neuroimaging. 2019;288:21–8.
3. Maggio N, Vlachos A. Tumor necrosis factor (TNF) modulates synaptic plasticity in a concentration-dependent manner through intracellular calcium stores. J Mol Med. 2018;96:1039–47.
4. Beattie EC, Stellwagen D, Morishita W, Bresnahan JC, Ha BK, Von Zastrow M, et al. Control of synaptic strength by glial TNFalpha. Science. 2002;295:2282–5.
5. Wei H, Zou H, Sheikh AM, Malik M, Dobkin C, Brown WT, et al. IL-6 is increased in the cerebellum of autistic brain and alters neural cell adhesion, migration and synaptic formation. J Neuroinflammation. 2011;8:52.
6. Stevens B, Allen NJ, Vazquez LE, Howell GR, Christopherson KS, Nouri N, et al. The classical complement cascade mediates CNS synapse elimination. Cell. 2007;131:1164–78.
7. Glynn MW, Elmer BM, Garay PA, Liu XB, Needleman LA, El-Sabeawy F, et al. MHCI negatively regulates synapse density during the establishment of cortical connections. Nat Neurosci. 2011;14:442–51.
8. Liang Q, Su L, Zhang D, Jiao J. CD93 negatively regulates astrogenesis in response to MMRN2 through the transcriptional repressor ZFP503 in the developing brain. Proc Natl Acad Sci USA. 2020;117:9413–22.
9. Zhang D, Liu C, Li H, Jiao J. Deficiency of STING signaling in embryonic cerebral cortex leads to neurogenic abnormalities and autistic-like behaviors. Adv Sci. 2020;7:2002117.
10. Chen G, Kim YH, Li H, Luo H, Liu DL, Zhang ZJ, et al. PD-L1 inhibits acute and chronic pain by suppressing nociceptive neuron activity via PD-1. Nat Neurosci. 2017;20:917–26.
11. Baruch K, Deczkowska A, Rosenzweig N, Tsitsou-Kampeli A, Sharif AM, Matcovitch-Natan O, et al. PD-1 immune checkpoint blockade reduces pathology and improves memory in mouse models of Alzheimer's disease. Nat Med. 2016;22:135–7.
12. Leroy C, Landais E, Briault S, David A, Tassy O, Gruchy N, et al. The 2q37-deletion syndrome: an update of the clinical spectrum including overweight, brachydactyly and behavioural features in 14 new patients. Eur J Hum Genet. 2013;21:602–12.
13. Zhao T, Gan Q, Stokes A, Lassiter RN, Wang Y, Chan J, et al. beta-catenin regulates Pax3 and Cdx2 for caudal neural tube closure and elongation. Development. 2014;141:148–57.
14. Han Y. Liu D, and Li L. PD-1/PD-L1 pathway: current researches in cancer. Am J Cancer Res. 2020;10:727–42.
15. Boulanger LM. Immune proteins in brain development and synaptic plasticity. Neuron. 2009;64:93–109.
16. Guilloux JP, Douillard-Guilloux G, Kota R, Wang X, Gardier AM, Martinowich K, et al. Molecular evidence for BDNF- and GABA-related dysfunctions in the amygdala of female subjects with major depression. Mol Psychiatry. 2012;17:1130–42.
17. Muller N, Schwarz MJ. The immune-mediated alteration of serotonin and glutamate: towards an integrated view of depression. Mol Psychiatry. 2007;12:988–1000.

18. Winter G, Hart RA, Charlesworth RPG, Sharpley CF. Gut microbiome and depression: what we know and what we need to know. Rev Neurosci. 2018;29:629–43.
19. Schmaal L, Hibar DP, Samann PG, Hall GB, Baune BT, Jahanshad N, et al. Cortical abnormalities in adults and adolescents with major depression based on brain scans from 20 cohorts worldwide in the ENIGMA Major Depressive Disorder Working Group. Mol Psychiatry. 2017;22:900–9.
20. Ji F, Wang W, Feng C, Gao F, Jiao J. Brain-specific Wt1 deletion leads to depressive-like behaviors in mice via the recruitment of Tet2 to modulate Epo expression. Mol Psychiatry. 2021;26:4221–33.
21. Li H, Zhu Y, Morozov YM, Chen X, Page SC, Rannals MD, et al. Disruption of TCF4 regulatory networks leads to abnormal cortical development and mental disabilities. Mol Psychiatry. 2019;24:1235–46.
22. Deng ZF, Zheng HL, Chen JG, Luo Y, Xu JF, Zhao G, et al. miR-214-3p targets beta-catenin to regulate depressive-like behaviors induced by chronic social defeat stress in mice. Cereb Cortex. 2019;29:1509–19.
23. Karege F, Perroud N, Burkhardt S, Fernandez R, Ballmann E, La Harpe R, et al. Protein levels of beta-catenin and activation state of glycogen synthase kinase-3beta in major depression. A study with postmortem prefrontal cortex. J Affect Disord. 2012;136:185–8.
24. Gould TD, O'Donnell KC, Picchini AM, Dow ER, Chen G, Manji HK. Generation and behavioral characterization of beta-catenin forebrain-specific conditional knockout mice. Behav Brain Res. 2008;189:117–25.
25. Chenn A, Walsh CA. Regulation of cerebral cortical size by control of cell cycle exit in neural precursors. Science. 2002;297:365–9.
26. Machon O, van den Bout CJ, Backman M, Kemler R, Krauss S. Role of beta-catenin in the developing cortical and hippocampal neuroepithelium. Neuroscience. 2003;122:129–43.
27. Li Y, Jiao J. Histone chaperone HIRA regulates neural progenitor cell proliferation and neurogenesis via beta-catenin. J Cell Biol. 2017;216:1975–92.
28. Geerlings MI, Sigurdsson S, Eiriksdottir G, Garcia ME, Harris TB, Sigurdsson T, et al. Associations of current and remitted major depressive disorder with brain atrophy: the AGES-Reykjavik Study. Psychol Med. 2013;43:317–28.
29. Lorenzetti V, Allen NB, Fornito A, Yucel M. Structural brain abnormalities in major depressive disorder: a selective review of recent MRI studies. J Affect Disord. 2009;117:1–17.
30. Videbech P, Ravnkilde B. Hippocampal volume and depression: a meta-analysis of MRI studies. Am J Psychiatry. 2004;161:1957–66.
31. Zhao J, Roberts A, Wang Z, Savage J, Ji RR. Emerging role of PD-1 in the central nervous system and brain diseases. Neurosci Bull. 2021;37:1188–202.
32. Zhao J, Bang S, Furutani K, McGinnis A, Jiang C, Roberts A, et al. PD-L1/PD-1 checkpoint pathway regulates hippocampal neuronal excitability and learning and memory behavior. Neuron. 2023;S0896-6273:00395-1. https://doi.org/10.1016/j.neuron.2023.05.022.

ACKNOWLEDGEMENTS

We thank all members of our lab for their valuable suggestions. We also thank Shiwen Li, Lijuan Wang, Hua Qin, and Xili Zhu for their help in confocal imaging and behavioral analysis. This work was supported by grants from the National Key R&D Program of China (2019YFA0110301 and 2021YFA1101402), the National Natural Science Foundation of China (32230040, 81825006, and 92149304), and Guangdong Basic and Applied Basic Research Foundation (2022B1515120026).

AUTHOR CONTRIBUTIONS

FJ performed the experiments, analyzed the results, and wrote the manuscript. CF constructed the plasmids of Pd1 and PdI1. JQ, CW, LS, WW, MZ, HL, LM, WL, CL, ZT, and BH provided help in the experiment performance. DZ provided help in human NSCs culture. FJ and JX supervised the project. JJ supervised the project and provided funding support.

COMPETING INTERESTS

The authors declare no competing interests.

ADDITIONAL INFORMATION

Supplementary information The online version contains supplementary material available at https://doi.org/10.1038/s41418-023-01203-3.

Correspondence and requests for materials should be addressed to Fen Ji, Fengzeng Jian, Jingdun Xie or Jianwei Jiao.